Antiviral Research 83 (2009) 80–85

Contents lists available at ScienceDirect

Antiviral Research

journal homepage: www.elsevier.com/locate/antiviral

Synthesis and anti-Hantaan virus activity of N^1-3-fluorophenyl-inosine

Dong-Hoon Chung[a], J. Jacob Strouse[b], Yanjie Sun[a], Jeffrey B. Arterburn[b], William B. Parker[a], Colleen B. Jonsson[a,*]

[a] Department of Biochemistry and Molecular Biology, Southern Research Institute, 2000 9th Ave South, Birmingham, AL 35205, United States
[b] Department of Chemistry, New Mexico State University, Las Cruces, NM 88003, United States

ARTICLE INFO

Article history:
Received 21 August 2008
Received in revised form 23 March 2009
Accepted 25 March 2009

Keywords:
Hantaan virus
Nucleosides
Ribavirin
Hantavirus

ABSTRACT

As part of an ongoing effort to develop new antiviral nucleoside analogs, our interest was drawn to N^1-aryl purines as a novel structural class and potential scaffold for drug discovery. Herein, we describe the synthesis of N^1-3-fluorophenyl-inosine (FPI) and N^1-3-fluorophenyl-hypoxanthine (FP-Hx) and their antiviral activity against hantaviruses. The EC_{50} for FPI and FP-Hx were 94 and 234 μM, respectively, against Hantaan virus. FPI was not toxic to mammalian cells at concentrations that exhibited antiviral activity. Analysis of its metabolism revealed a low conversion of FPI in Vero E6 or human cells to a 5′-triphosphate, and it was a poor substrate for human purine nucleoside phosphorylase. Further, the compound did not alter GTP levels indicating FPI does not inhibit inosine monophosphate dehydrogenase. With respect to the virus, FPI did not decrease viral RNA levels or increase the mutation frequency of the viral RNA. This suggests that the antiviral activity of FPI might be solely due to the interaction of FPI or its metabolites with viral or host proteins involved in post-replication events that would affect the levels of infectious virus released. Synthesis of other compounds structurally similar to FPI is warranted to identify more potent agents that selectively abrogate production of infectious virus.

1. Introduction

Hantaviruses are enzootic viruses of wild rodents in which they cause persistent infections without apparent disease symptoms in their natural hosts (Botten et al., 2003; Meyer and Schmaljohn, 2000a,b; Netski et al., 1999; Yanagihara et al., 1985). When transmitted to humans, however, several members of the genus cause deadly illnesses such as hemorrhagic fever with renal syndrome (HFRS) and hantavirus pulmonary syndrome (HPS) (Peters et al., 1999; Schmaljohn and Hjelle, 1997). Old world hantaviruses such as Hantaan virus (HTNV) cause the vast majority of HFRS cases in Asia and Europe, whereas new world hantaviruses are responsible for HPS cases in the Americas. With respect to vaccines, immunotherapeutics or antivirals, only ribavirin (1-β-D-ribofuranosyl-1,2,4-triazole-3 carboxamide, RBV) has been explored in the treatment of human infections (Chapman et al., 1999; Huggins et al., 1991; Mertz et al., 2004). RBV is not FDA-approved for the prophylaxis or treatment of hantaviral infections at this time.

Hantaviruses are enveloped, spherical, negative-strand RNA viruses with a tripartite, segmented genome composed of S (small), M (medium) and L (large) RNAs (Schmaljohn and Hooper, 2001). These segments encode the nucleocapsid or N protein, two glycoproteins, Gn and Gc, and the RNA dependent RNA polymerase (RdRp) or L protein, respectively. The viral L protein mediates both the replication and transcription of viral RNAs in the cytoplasm and represents an attractive target for nucleoside-based antivirals. Previously, we have reported the antiviral activity of RBV for HTNV derives from inhibition of inosine monophosphate dehydrogenase (IMPDH) and an increase in mutation frequency in the viral genome (Sun et al., 2007; Chung et al., 2007).

Nucleoside and nucleobase analogs are an important class of antiviral drugs. Arylation of the purine heterocyclic base dramatically affects the steric environment, polarity, hydrogen bonding and π-stacking capacities associated with base-pairing, and protein receptor binding. N^2-Phenyl-dGTP derivatives are potent and selective inhibitors of DNA polymerases (Wright and Brown, 1990), and acyclic N^2-phenyl-guanine derivatives are inhibitors of HSV thymidine kinases (Manikowski et al., 2005). Inosine nucleotides possessing electron-deficient aryl substituents at the 8- or 2-position are inhibitors of IMPDH (Skibo and Meyer, 1981; Wong and Meyer, 1984). Purine nucleosides possessing six and five-membered heterocycles substituted at the 6-position (such as 6-(1H-pyrrol-3-yl)-9-(β-D-ribofuranosyl)purine) have exhibited potent cytotoxic and anti-HCV activity (using a HCV subgenomic replicon assay) (Hocek et al., 2005). As part of an ongoing effort to develop new antiviral nucleosides, our interest was drawn to N^1-aryl purines as a novel structural class and potential scaffold

* Corresponding author. Tel.: +1 205 581 2681; fax: +1 205 581 2093.
E-mail address: jonsson@sri.org (C.B. Jonsson).

0166-3542/$ – see front matter © 2009 Elsevier B.V. All rights reserved.
doi:10.1016/j.antiviral.2009.03.007

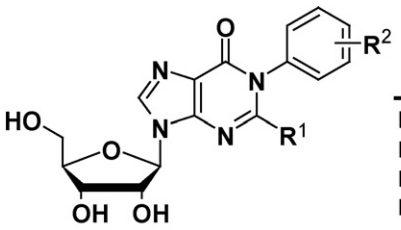

	R^1	R^2
FPI	H	3-F
MPI	H	4-OMe
NPI	H	3-NO_2
MPG	NH_2	4-OMe

Fig. 1. Structure of N^1-aryl purines.

for drug discovery (Fig. 1) (Strouse et al., 2005 ACS). We recently described a synthetic approach for copper-mediated N^1-arylation of protected purine nucleosides that provides convenient access to this structurally unique compound class (Strouse et al., 2005). Herein, we describe (1) the antiviral activity of this novel class of N^1-aryl purine analogs against HTNV, (2) the metabolism of these compounds in Vero E6 and CEM cells, and (3) determination of the mutation frequency of and levels of the viral RNA.

2. Materials and methods

2.1. Syntheses

All reactions were performed in an efficient fume hood. Solvents and reagents were purchased from Thermo Fisher (Hampton, NH) and Sigma–Aldrich (St. Louis, MO) and were used without further purification unless noted. Preparative chromatography was performed using medium pressure flash chromatography (Sorbent Technologies, Atlanta, GA). Deuterated solvents were used without further purification. NMR spectra were acquired at ambient temperatures ($18 \pm 2\,^{\circ}C$) unless otherwise noted. The ^1H NMR spectra were referenced to solvent. The ^{13}C $\{^1H\}$ NMR spectra were recorded at 100 MHz and referenced relative to the ^{13}C $\{^1H\}$ peaks of the solvent. Spectra are reported as (ppm), (multiplicity, coupling constants (Hz), and number of protons). Coupling to fluorine is given in ^{13}C NMR and noted in parenthesis after the chemical shift. Infrared spectra were recorded as KBr pellets and are reported in cm^{-1}. Mass spectra showing the presence of a molecular ion were obtained using electrospray ionization (MS-ESI) or atmospheric pressure chemical ionization (MS-API) in positive mode. Combustion analysis was carried out by Desert Analytics (Tucson, AZ). The starting 2′,3′,5′-tris-(O-tert-butyldimethylsilyl)-protected nucleosides were prepared by standard conditions from inosine or guanosine and *tert*-butyldimethylsilyl chloride.

N^1-3-fluorophenyl-2′,3′,5′-tris-(O-tert-butyldimethylsilyl)-inosine (***TBS-FPI***). To an oven dried Schlenk tube was added 2′,3′,5′-tris-(O-tert-butyldimethylsilyl)-inosine (TBS-I) (2.4 g, 4.0 mmole), 3-fluorophenylboronic acid (1.1 g, 8.0 mmole), anhydrous $Cu(OAc)_2$ (800 mg, 4.4 mmole), pyridine-N-oxide (800 mg, 4.0 mmole), ground 4 Å molecular sieves (∼1 g), and a stir bar. The tube was then sealed with a rubber septa, evacuated and flushed with oxygen. Dry pyridine (647 ml, 8.0 mmole) and CH_2Cl_2 (20 ml) were then added and the reaction was stirred vigorously at r.t. for 24 h. The reaction was then quenched with 10% NH_4OH/MeOH (5 ml), then diluted with hexanes (500 ml). The combined organics were washed with successive 250 ml portions of water, sat. NH_4Cl, 1 M NaCl, and sat. NaCl. The organic layer was dried (Na_2SO_4), concentrated *in vacuo* and purified by medium pressure flash chromatography with CH_2Cl_2/MeOH as eluent, yielding an amorphous white solid (1.93 g, 2.74 mmole, 67%) FT-IR (PTFE card, cm^{-1}) 1716; ^1H NMR (400 MHz, $CDCl_3$) δ 8.20 (1H, s), 7.99 (1H, s), 7.45 (1H, m), 7.16–7.13 (3H, m), 5.99 (1H, d, J = 4.8 Hz), 4.46 (1H, m), 4.29 (1H, m), 4.11 (1H, m), 3.97 (1H, m), 3.77 (1H, m), 0.93–0.80 (27H, mult. s), 0.12–0.16 (18H, mult. s); ^{13}C NMR (400 MHz, $CDCl_3$) δ 162.6 (J = 248.1 Hz), 156.0, 147.1, 146.4, 138.4 (J = 9.5 Hz), 130.7 (J = 9.0 Hz), 124.7, 123.0, 116.3 (J = 20.0 Hz), 115.2 (J = 23.9 Hz), 88.1, 85.4, 76.7, 71.6, 62.3, TBS-not listed; Elem. Anal. Calcd. For $C_{34}H_{57}FN_4O_5Si_3$: C, 57.92; H, 8.15; N, 7.95 Found: C, 57.94; H, 8.36; N, 7.83.

N^1-3-fluorophenyl-inosine (FPI). A 5.0 ml solution of 1 M tetrabutylammonium fluoride in THF was added to a cooled (−10 °C) solution of TBS-FPI (1.06 g, 1.5 mmole) in dry THF (25 ml), and stirred 1.5 h. The reaction mixture was directly loaded on a 5 cm diameter column (∼350 ml of 70–230 mesh 60 Å silica gel) and eluted with acetone to remove the tetrabutylammionum salts. The eluted fractions were concentrated, and the resulting solid was purified by medium pressure flash chromatography with toluene/EtOH as eluent to yield an amorphous white solid (469 mg, 1.29 mmole, 86%) FT-IR (KBr, cm^{-1}) 3394, 2931, 1699, 1601, 1578, 1546, 1489, 1226; ^1H NMR (CD_3OD, 400 MHz) δ 8.39 (1H, s), 8.30 (1H, s), 7.57 (1H, m), 7.35–7.26 (3H, m), 6.04 (1H, d, J = 5.9 Hz), 4.63 (1H, m), 4.33 (1H, m), 4.13 (1H, m), 3.86 (1H, m), 3.75 (1H, m); ^{13}C NMR (CD_3OD, 400 MHz) δ 164.1 (J = 245.4 Hz), 157.9, 149.2, 148.7, 141.5, 139.9 (J = 10.2 Hz), 132.1 (J = 8.7 Hz), 125.3, 124.8 (J = 2.3 Hz), 117.4 (J = 21.2 Hz), 116.4 (J = 23.9 Hz), 90.4, 87.5, 76.3, 72.0, 62.9. MS-ESI calcd for $C_{16}H_{15}FN_4O_5$ $[M+1]^+$ 363.11 m/z, found 363.26 m/z. The related N^1-4-methoxyphenyl-(MPI), 3-nitrophenylinosine (NPI), and 4-methoxyphenylguanosine (MPG) analogs were prepared following this same general procedure.

N^1-3-fluorophenyl-hypoxanthine (FP-Hx). To a pressure tube was added a stir bar and TBS-FPI (378 mg, 0.54 mmole). This was dissolved in MeOH (5 ml), followed by addition of 2 M HCl (10 ml). The tube was then sealed and heated at 95 °C for 2 h and then cooled to room temperature. The solution was quenched with $NaHCO_3$ and diluted with water followed by extraction with 3 portions EtOAc. The organics were dried over Na_2SO_4 and evaporated *in vacuo* followed by medium pressure flash chromatography with MeOH/CH_2Cl_2 as eluent. The solids were then recrystallized from acetone yielding a white solid (63 mg, 0.27 mmole, 51%). FT-IR (KBr, cm^{-1}) 1706; ^1H NMR (CD_3OD, 400 MHz) δ 8.26 (1H, s), 8.17 (1H, s), 7.59 (1H, m), 7.32 (3H, m); MS-API calcd for $C_{11}H_7FN_4O$ $[M+1]^+$ 231.07 m/z, found 231.06 m/z.

Radiolabeled compounds. N^1-3-fluorophenyl-[8-^{3}H]inosine ([^{3}H]FPI) was prepared by Moravek Biochemicals, Inc. (Brea, CA) with radiochemical purity ≥97% by HPLC and specific activity ≥ 10 mCi/mmole. N^1-3-fluorophenyl-[8-^{3}H]hypoxanthine ([^{3}H]FP-Hx) was prepared from [8-^{3}H]FPI using *E. coli* purine nucleoside phosphorylase. Both radiolabeled compounds were purified using reverse phase HPLC before use in these studies. The column used for purification was a 5 μm, 150 mm × 4.6 mm BDS Hypersil C-18 column (Thermo Electron Corp., Bellefonte, PA), and the mobile phase was a 5–50% acetonitrile gradient in 50 mM ammonium dihydrogen phosphate buffer (pH 4.5) for 30 min at a flow rate of 1 ml/min.

2.2. Antiviral activity assays

The anti-hantaviral activity of compounds was evaluated by a plaque reduction assay in Vero E6 cells (ATCC CRL-1587) infected with HTNV (strain 76–118) or ANDV (strain Chile-9717869, from T. Ksiazek, CDC, Atlanta) using the method as previously described (Chung et al., 2008). Three days old confluent Vero E6 cells grown in 6-well cell culture plate were infected with HTNV at a multiplicity of infection (MOI) of 0.1 by adsorption for 1 h. After removal of virus, media was replaced with DMEM containing 10% FBS containing antiviral compounds, and the cells were incubated further at 37 °C with 5% CO_2. Cell supernatants were harvested from each well 3 days after infection or as indicated in figure legends or text. Cell supernatants were subjected to plaque assay to measure the plaque-forming unit (PFU) of progeny virus released into the supernatant.

Viral S segment genomic RNA levels were measured by using a quantitative real-time RT-PCR method described previously (Chung et al., 2007; Sun et al., 2007). Briefly, viral S genome cDNAs were synthesized from 0.2 μg of total RNA isolated from cells infected with HTNV for 3 days. cDNA was synthesized with 10 pmole of vhRT primer (5′-TAGTAGTAGACTCCCTAAAGAGCT-3′) for the S segment of the vRNA and 10 pmole of 18SRT primer (5′-TCTTCTCAGCGCTCCGCCA-3′) for the endogenous control of 18S rRNA. The HTNV replicon (232–322 nucleotides in S segment RNA) was measured using the TaqMan probe, which was labeled with either the reporter dye (6-carboxylfluorescein (FAM™) at 5′ end) or the minor grove binder at the 3′ end. QRT-PCR was performed in triplicate and the amount of HTNV S segment was calculated by using the comparative CT, $2^{-\Delta\Delta Ct}$ method.

2.3. Measurement of mutation frequency

The mutation frequency was measured as recently described (Chung et al., 2007). Briefly, HTNV S segment cDNAs were amplified from 0.2 μg of total RNA isolated from cells infected with HTNV for 3 days with Phusion™ High-Fidelity DNA Polymerase (Finnzyme Oy, Finland) and cloned into plasmid (TOPO® Cloning Kits for Sequencing, Invitrogen). Individual plasmid DNA from 96 colonies was subjected to DNA sequencing, and mutation analysis was performed with SeqScape program (Applied Biosystems) by comparing the published HTNV S segment sequence from 91–1329 nt of the sense strand (GenBank accession number M14626) with cDNAs isolated from untreated and treated cells.

2.4. Determination of toxicity to CEM cells

Wild-type CEM cells (human leukemia cell line; American Type Culture Collection, Manassas, VA) were grown in RPMI 1640 medium (Invitrogen, Carlsbad, CA) containing 10% fetal bovine serum (Atlanta Biologicals, Norcross, GA), 1 mg/ml sodium bicarbonate, 10 U/ml penicillin, 10 μg/ml streptomycin, and 50 μg/ml gentamycin. The effect of compound on CEM cell growth was determined by counting cell numbers with a coulter counter.

2.5. Measurement of intracellular FPI metabolites and natural nucleotides

Confluent Vero E6 cells and exponential dividing CEM cells were incubated at 37 °C with [^{3}H]FPI or [^{3}H]FP-Hx. Intracellular FPI metabolites and natural nucleotides (ATP and GTP) were measured using anion exchange HPLC as described (Parker et al., 1998). The natural nucleotides (ATP and GTP) were detected by measurement of the UV absorbance at 260 nm, and radioactive metabolites of FPI were detected by counting 1-min fractions. Intracellular ATP levels were used as a measure of the number of cells. None of the treatments shown in the current work resulted in changes to ATP levels.

3. Results

3.1. Chemistry

The cuprous acetate mediated N^1-arylation of the TBS-protected purines with substituted phenylboronic acids provided the desired

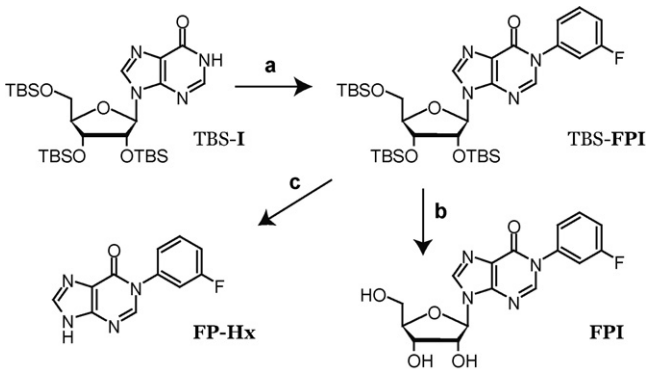

Fig. 2. Synthesis of N^1-3-fluorophenyl-purine analogs. Reagents: (a) 3-fluorophenylboronic acid, cupric acetate, pyridine-N-oxide, pyridine, 4 Å molecular sieves, oxygen, CH_2Cl_2; (b) tetrabutylammonium fluoride, THF, −10 °C; (c) 2 M HCl, methanol, 95 °C.

N^1-aryl purine derivatives (FPI, MPI, NPI, and MPG) in good yield (Figs. 1 and 2) (Strouse et al., 2005). The subsequent removal of the TBS-ether protecting groups was achieved with tetrabutylammonium fluoride in THF at −10 °C. Reduced temperature was necessary to avoid uncharacterized degradation that generated by-products. Preparative medium pressure chromatography utilizing toluene/ethanol as eluent was effective for complete removal of the tetrabutylammonium salts as recently described (Dong and Paquette, 2005). The N^1-3-fluorophenyl-hypoxanthine base derivative **FP-Hx** was obtained by acidic cleavage of the protected sugar moiety in methanolic HCl.

3.2. Antiviral activity of FPI against hantaviruses

The compounds shown in Fig. 1 were assessed for antiviral activity for HTNV using a plaque assay after 1–3 day incubation with each compound. FPI (3-fluoro) and NPI (3-nitro) gave a log reduction in plaque, comparably to RBV. The 3-nitrophenyl derivative, NPI, was more potent, however, FPI was selected for further evaluation in order to avoid potential complications due to possible biochemical reduction of the nitro group in NPI (Table 1).

The anti-HTNV activity of FPI was evaluated over a 3-day period at a single dose (138 μM) in comparison with RBV at 40 μM (Fig. 3). RBV inhibited production of infectious progeny virus showing a reduction in pfu/ml of 90% and 94% on days 1 and 3, respectively. Interestingly FPI showed a different pattern of inhibition kinetics as compared to that of RBV over the three-day time period examined in that it increased over time. FPI showed a 35% and 73% reduction on day 1 and day 2, and finally, an approximate 80% reduction (0.72 log reduction) was observed at day 3 after treatment.

These results led us to evaluate the activity of the N-1-arylhypoxanthine, FP-Hx, (nucleobase form of FPI). The antiviral effect of FP-HX was evaluated in a dose response assay in a range of 100–868 μM. Response of FP-HX was weaker than FPI but significant (39% and 71% inhibition at 217 and 434 μM; 3 days post infection). The EC_{50} for FPI and FP-HX for HTNV were 94 and 234 μM, respectively (Table 2). We evaluated the activity of FPI against ANDV using similar methods. We did not detect any antiviral activity of FPI against ANDV in a concentration range from 27 to

Table 1
Anti-HTNV activity of FPI and NPI in single dose treatment.

	Mock	FPI (138 μM)	NPI (129 μM)	Ribavirin (41 μM)
Progeny virus titer (per ml)	1.1×10^5	8.0×10^3	1.3×10^3	4.6×10^3

Vero E6 cells were infected with HTNV, 76–118 in a complete media and then cultured in a complete media with compounds as indicated. The media from day 1 were harvested and the progeny viruses there were titrated.

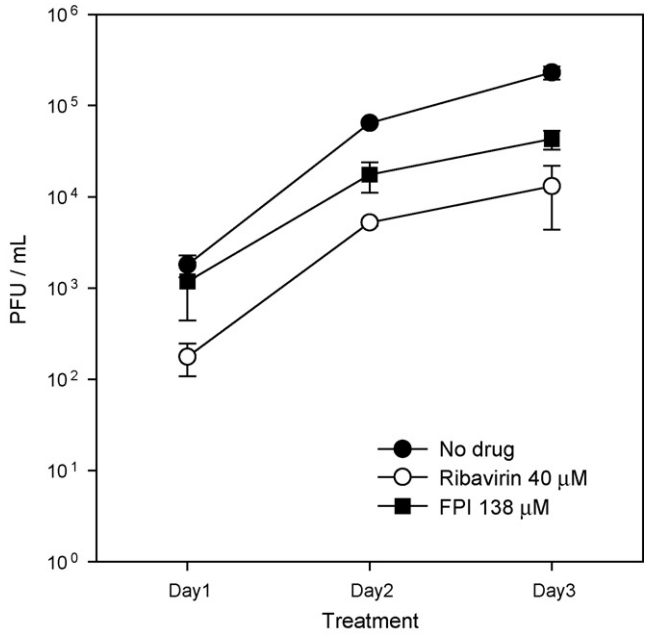

Fig. 3. Inhibition of virus production by FPI. Vero E6 cells infected with HTNV were treated with either 138 μM (50 μg/ml) of FPI or 40 μM of RBV and the titers of progeny virus were determined in the supernatant. Each number represents the mean ± standard deviation from 2 independent experiments with triplicates of titration results.

Table 2
Efficacy of FPI and FPI-Hx against hantaviruses and the selective index 50.

	EC_{50} (μM) against		CC_{50} in CEM cells (μM)	SI_{50} for HTNV
	HTNV	ANDV		
FPI	94	>138	>270	>3
FPI-Hx	234	NT	>434	>1.85

NT: not tested.
EC_{50}, 50% inhibitory concentration or concentration required to inhibit virus yield at 72 h p.i. by 50%.

276 μM following a 3 day incubation period of virus in the presence of compound.

We tested the compounds in CEM cells as described above to provide additional insight into cytotoxicity. Concentrations of FPI as high as 270 μM did not affect the growth of CEM cells, which revealed that FPI was not toxic to CEM cells. Since the concentration of FPI required to inhibit CEM cell growth by 50% (CC_{50}) was higher than 270 μM, the selective index for FPI was greater than >3.

We measured the copy number of viral RNA (Table 3) in Vero E6 cells infected with HTNV and treated with FPI using a real-time PCR assay. Our objective was to ascertain if the compound decreased the synthesis of viral RNA by the polymerase. Intriguingly, we observed no significant decrease in levels of viral RNA in FPI-treated versus RBV-treated Vero E6 cells infected with HTNV.

Table 3
Effect of FPI and RBV on viral RNA copy number.

	Concentration (μM)	Relative vRNAc
FPI	69	1.34
	552	1.13
RBV	41	0.24
	164	0.01

HTNV infected cells were treated with FPI or RBV at the indicated concentrations and relative viral S segment RNA was measured and compared with mock-infected samples using, $2^{-\Delta\Delta Ct}$ method normalized with 18S RNA Ct values.

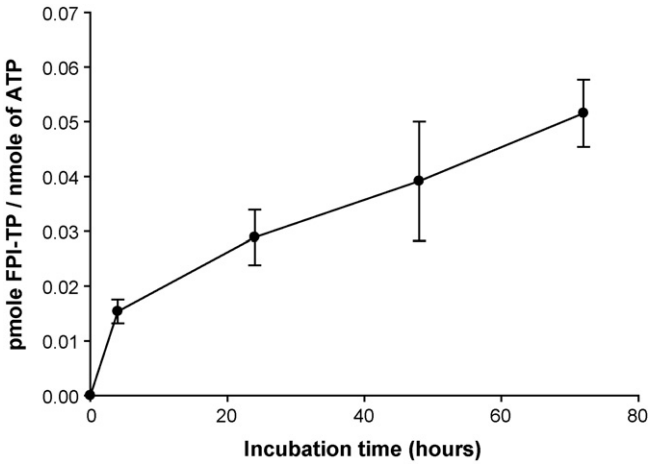

Fig. 4. Metabolism of FPI in Vero E6 cells. Vero E6 cells were treated with 27 μM [^{3}H]FPI for 4, 24, 48, or 72 h. Acid-soluble extracts of the cell pellets were analyzed by strong anion exchange (SAX) HPLC to determine the amount of intracellular FPI-TP and ATP. Each number represents the mean ± SD from 3 measurements.

3.3. Metabolism and biochemical activity of FPI

Tritium-labeled [^{3}H]FPI was obtained and its metabolism was evaluated in confluent Vero E6 cell cultures to determine the active state of the molecule. A small peak of radioactivity was detected that eluted from the SAX HPLC column in the triphosphate region that was close to the limit of detection. At best only 0.3 pmoles of FPI-triphosphate (FPI-TP) were formed in Vero E6 cells treated with 27 μM FPI for 4 h, which was only 0.002% of the amount of intracellular ATP that was in the Vero E6 cells (0.02 pmoles of FPI-TP per nmole of ATP). The intracellular concentration of FPI-TP continued to rise over the 72 h incubation period to 0.05 pmoles of FPI-TP/nmole of ATP (Fig. 4). Since the intracellular concentration of ATP is approximately 3 mM (Jones, 1980), these results indicated that the intracellular concentration of FPI-TP was approximately 0.15 μM after 72 h of incubation with 27 μM FPI. Increasing the extracellular concentration of FPI from 27 to 270 resulted in a 10-fold increase in intracellular levels of FPI-TP (data not shown), which suggests that the metabolism of FPI was not saturated in Vero E6 up to a concentration of 270 μM. We have previously shown that treatment of Vero E6 cells with 41 μM RBV for 4 h results in 13 pmole of RBV-TP/nmole ATP (Sun et al., 2007), and hence, the rate of metabolism of RBV in Vero cells is approximately 600-fold greater than FPI.

To confirm the low level of conversion of FPI to a triphosphate form, we examined the metabolism of FPI in CEM cells, a human T cell lymphoma cell line. Incubation of 3×10^7 CEM cells with 27 μM of FPI for 4 h resulted in the production of 7 pmoles of FPI-TP, or 0.23 pmoles FPI-TP per 10^6 cells (or a concentration of 0.23 μM assuming that that the volume of 10^6 cells is 1 μl). For comparison, incubation of CEM cells with 41 μM RBV resulted in 91 pmoles of RBV-TP per 10^6 cells, a concentration that was 400-fold greater than FPI-TP that was formed. These results agreed with those obtained

Table 4
FPI and RBV as substrates for human and *E. coli* purine nucleoside phosphorylase.

	Inosine	FPI (nmoles/mg-hr)	RBV
Human PNP	370,000 ± 38,000	2 ± 0.2	80 ± 2
E. coli PNP	620,000 ± 17,000	53,000 ± 3,000	30 ± 17

Human and *E. coli* PNP were incubated with 100 μM inosine, FPI, or RBV at protein concentrations that resulted in linear production of product. Substrate was separated from product using reverse phase HPLC and the rate of the reaction was determined. The numbers presented are the mean ± standard deviations of 3 separate measurements.

Table 5
Mutational frequency analysis.

		No drug	RBV[a]	FPI[b]
Analyzed nucleotides		116,466	115,227	113,988
Mutation frequency[c]	C → U, G → A	0.2	2.3	0.4
	U → C, A → G	0.7	0.4	0.3
	Others[d]	0.2	0.6	0.9
	Total	1.0	3.3	1.1
% of C → U, G → A in mutations		16.7%	68.4%	33.3%
Non-synonymous substitutions/point mutations		5/10	24/34	7/9
Number of cDNAs		94	93	92
% of cDNA with mutation		11.7%	32.3%	13.0%

[a] Ribavirin at 81 μM.
[b] FPI at 270 μM.
[c] Mutations per 10,000 nucleotides.
[d] Transversion and frame shift mutations.

in Vero cells and indicate that FPI was poorly metabolized in mammalian cells. [^{3}H]FP-Hx was also metabolized in CEM cells, but at a rate that was approximately 30% that of [^{3}H]FPI (data not shown).

The extracellular concentration of FPI was stable in the CEM cell cultures over a 72 incubation period. Since guanosine was rapidly cleared from the cell culture, the stability of FPI shows that it was not a good substrate for mammalian purine nucleoside phosphorylase (PNP). Incubation with purified enzyme supported this conclusion (Table 4). Human PNP cleaved inosine at a rate that was 185,000 times faster than that of FPI. Interestingly, FPI was a relatively good substrate for *E. coli* PNP. It was cleaved at 10% the rate of inosine. RBV was a poor substrate for both enzymes.

Treatment with 270 μM FPI did not affect intracellular GTP levels during 72 h of incubation (Fig. 5), which indicated that neither FPI nor its metabolites inhibited IMP dehydrogenase activity.

3.4. FPI effect on the mutation frequency and chain termination

We have previously shown that RBV causes error-prone replication and an increase in mutation frequency in the HTNV genome (Chung et al., 2007; Severson et al., 2003). To explore this as a possible mechanism for the antiviral activity of FPI, we cloned and sequenced cDNAs of viral RNA and analyze

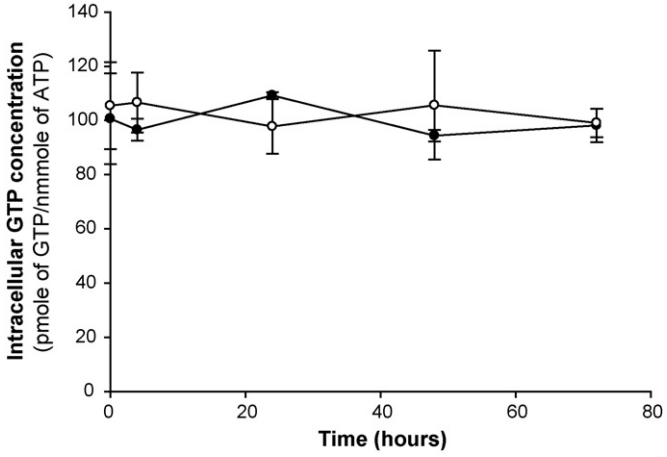

Fig. 5. Treatment of Vero E6 cells with FPI did not affect intracellular GTP levels. Vero E6 cells were treated with 270 μM of FPI(●) or no drug (○) for 0, 4, 24, 48, or 72 h and the acid-soluble extracts of cell pellets from cell cultures were analyzed by strong anion exchange (SAX) HPLC to determine intracellular GTP and ATP concentrations. Each number represents the mean ± SD from 3 measurements.

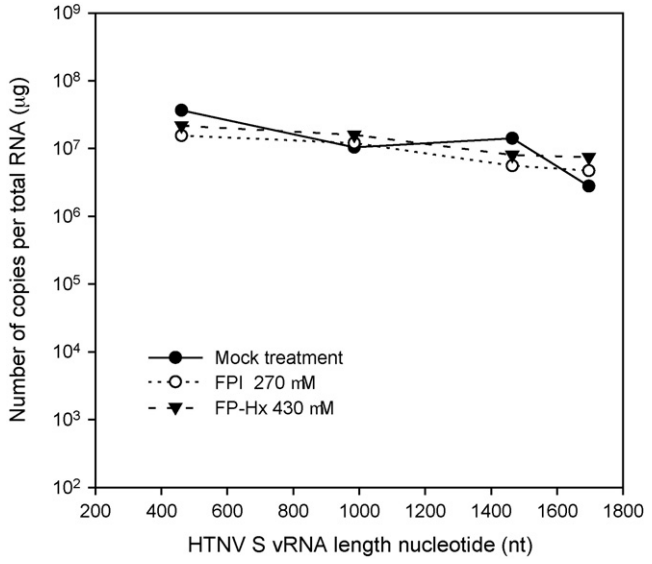

Fig. 6. Treatment of Vero E6 cells with FPI did not affect viral RNA length profile. Vero E6 cells were treated with 270 μM of FPI(○), 434 μM of FP-HX (▼)or no drug (●) for 3 days and the RNA was extracted. cDNAs were synthesized from 4 different primers, which recognize corresponding locations in HTNV S RNA and then cDNA was copy number was measured by qRT-PCR.

d mutation frequency following treatment for 3 days with FPI (270 μM) or RBV (80 μM). We could not find any significant difference in the mutation frequency between the mock-treated and the FPI treated virus (Table 5).

We also asked whether the antiviral activity from FPI was due to early chain termination of the viral RNA during synthesis. We measured levels of the HTNV S segment cDNAs primed from different locations. At the concentration of 276 μM of FPI and 434 μM of FP-HX, there were no significant differences between control and treatments samples in copy number levels (Fig. 6).

4. Discussion

Herein, we describe the synthesis of the N^1-aryl purines, N^1-3-fluorophenyl-inosine (FPI) and N^1-3-fluorophenyl-hypoxanthine (FP-Hx), and show their antiviral activity against HTNV, but not ANDV. We have also tested FPI, FPI-HX and NPI against West Nile virus (strain NY-99), however the activities against West Nile virus were negligible (Data not shown). As compared to the antiviral, RBV,

which showed a constant and rapid antiviral effect in HTNV particle production, FPI showed an initial delay followed by increasing antiviral activity. The appearance of phosphorylated metabolites of FPI and FP-Hx in cells suggest that these metabolites could be involved in the antiviral activity of FPI. The slow onset of antiviral activity was consistent with the low metabolism of FPI in mammalian cells to a triphosphate form. In general, the relative rates of phosphorylation of FPI and FP-Hx correlated with their relative antiviral activities. However, the levels of viral RNA produced in the cell were not significantly lowered by FPI. Further, mutation analysis of the HTNV genome after treatment with FPI clearly showed that FPI is not a RNA mutagen. Using an assay that detects truncated viral RNAs, we found no evidence of chain-termination. Therefore, this strongly suggests that FPI is not incorporated into nascent viral RNAs. In addition, FPI did not affect intracellular GTP levels, and therefore, its mechanism of action does not involve the inhibition of IMPDH. If FPI-TP is responsible for the antiviral activity of FPI, this result indicates that FPI-TP may potently interact with the viral polymerase. If true, then prodrug approaches designed to increase intracellular metabolites of FPI should result in agents with more potent antiviral activity. However, because of the very low intracellular concentrations of FPI-TP that accumulated in mammalian cells, it is still possible that FPI-TP might not be responsible for the antiviral activity of FPI and that FPI and FP-Hx may be active without metabolism against later stages of the virus life cycle due to direct interaction with viral or host cell proteins.

The antiviral activity of nucleobase, FP-HX, was also demonstrated herein to be less active than nucleoside, FPI. This indicates that the activity is either (i) associated with the unique N^1-aryl purine structure; or (ii) the nucleobase is converted to a phosphorylated riboside as an active metabolite. The latter indicates the potential for additional synthetic modification of the N^1-aryl purine scaffold for optimization of antiviral activity against HTNV.

It is not yet clear which enzymes are involved in the metabolism of FPI. Based on the very low activity of FPI as a substrate for PNP and the fact that FP-Hx was less potent than FPI, it is unlikely that FPI was cleaved to FP-Hx prior to activation. Phosphorylation by nucleoside kinases is typically the first step in activation of nucleoside analogs. RBV is rapidly phosphorylated by adenosine kinase and subsequently converted to the triphosphate as the major metabolite in cells. N^1-aryl modification of inosine is expected to affect processing by host enzymes. Because FPI is an inosine analog, it is possible, if not likely, that it is a substrate for 5′-nucleotidase. Other enzymes that could be involved in its metabolism are adenosine kinase, adenosine phosphotransferase, or nicotinamide ribose kinase, and studies are currently under way to define the mechanistic pathway involved in its phosphorylation.

Acknowledgements

This work was supported by Department of Defense USAMRC grant number W81XWH-04-C-0055 (PI Jonsson), and NIH R21AI053304-02 (JA).

References

Botten, J., Mirowsky, K., Kusewitt, D., Ye, C., Gottlieb, K., Prescott, J., Hjelle, B., 2003. Persistent Sin Nombre virus infection in the deer mouse (Peromyscus maniculatus) model: sites of replication and strand-specific expression. J. Virol. 77, 1540–1550.

Chapman, L.E., Mertz, G.J., Peters, C.J., Jolson, H.M., Khan, A.S., Ksiazek, T.G., Koster, F.T., Baum, K.F., Rollin, P.E., Pavia, A.T., Holman, R.C., Christenson, J.C., Rubin, P.J., Behrman, R.E., Bell, L.J., Simpson, G.L., Sadek, R.F., 1999. Intravenous ribavirin for hantavirus pulmonary syndrome: safety and tolerance during 1 year of open-label experience. Ribavirin study group. Antivir. Ther. 4, 211–219.

Chung, D.H., Kumarapperuma, S.C., Sun, Y., Li, Q., Chu, Y.K., Arterburn, J.B., Parker, W.B., Smith, J., Spik, K., Ramanathan, H.N., Schmaljohn, C.S., Jonsson, C.B., 2008. Synthesis of 1-β-D-ribofuranosyl-3-ethynyl-[1,2,4]triazole and its in vitro and in vivo efficacy against Hantavirus. Antivir. Res. 79, 19–27.

Chung, D.H., Sun, Y., Parker, W.B., Arterburn, J.B., Bartolucci, A., Jonsson, C.B., 2007. Ribavirin reveals a lethal threshold of allowable mutation frequency for Hantaan virus. J. Virol. 81, 11722–11729.

Dong, S., Paquette, L.A., 2005. Stereoselective synthesis of conformationally constrained 2′-deoxy-4′-thia beta-anomeric spirocyclic nucleosides featuring either hydroxyl configuration at C5′. J. Org. Chem. 70, 1580–1596.

Hocek, M., Naus, P., Pohl, R., Votruba, I., Furman, P.A., Tharnish, P.M., Otto, M.J., 2005. Cytostatic 6-aryl purine nucleosides. 6. SAR in anti-HCV and cytostatic activity of extended series of 6-hetarylpurine ribonucleosides. J. Med. Chem. 48, 5869–5873.

Huggins, J.W., Hsiang, C.M., Cosgriff, T.M., Guang, M.Y., Smith, J.I., Wu, Z.O., LeDuc, J.W., Zheng, Z.M., Meegan, J.M., Wang, Q.N., et al., 1991. Prospective, double-blind, concurrent, placebo-controlled clinical trial of intravenous ribavirin therapy of hemorrhagic fever with renal syndrome. J. Infect. Dis. 164, 1119–1127.

Jones, M.E., 1980. Pyrimidine nucleotide biosynthesis in animals: genes, enzymes, and regulation of UMP biosynthesis. Annu. Rev. Biochem. 49, 253–279.

Manikowski, A., Verri, A., Lossani, A., Gebhardt, B.M., Gambino, J., Focher, F., Spadari, S., Wright, G.E., 2005. Inhibition of herpes simplex virus thymidine kinases by 2-phenylamino-6-oxopurines and related compounds: structure-activity relationships and antiherpetic activity in vivo. J. Med. Chem. 48, 3919–3929.

Mertz, G.J., Miedzinski, L., Goade, D., Pavia, A.T., Hjelle, B., Hansbarger, C.O., Levy, H., Koster, F.T., Baum, K., Lindemulder, A., Wang, W., Riser, L., Fernandez, H., Whitley, R.J., 2004. Placebo-controlled, double-blind trial of intravenous ribavirin for the treatment of hantavirus cardiopulmonary syndrome in North America. Clin. Infect. Dis. 39, 1307–1313.

Meyer, B.J., Schmaljohn, C., 2000a. Accumulation of terminally deleted RNAs may play a role in Seoul virus persistence. J. Virol. 74, 1321–1331.

Meyer, B.J., Schmaljohn, C.S., 2000b. Persistent hantavirus infections: characteristics and mechanisms. Trends Microbiol. 8, 61–67.

Netski, D., Thran, B.H., St Jeor, S.C., 1999. Sin Nombre virus pathogenesis in Peromyscus maniculatus. J. Virol. 73, 585–591.

Parker, W.B., Allan, P.W., Shaddix, S.C., Rose, L.M., Speegle, H.F., Gillespie, G.Y., Bennett Jr., L.L., 1998. Metabolism and metabolic actions of 6-methylpurine and 2-fluoroadenine in human cells. Biochem. Pharmacol. 55, 1673–1681.

Peters, C.J., Simpson, G.L., Levy, H., 1999. Spectrum of hantavirus infection: hemorrhagic fever with renal syndrome and hantavirus pulmonary syndrome. Annu. Rev. Med. 50, 531–545.

Schmaljohn, C., Hjelle, B., 1997. Hantaviruses: a global disease problem. Emerg. Infect. Dis. 3, 95–104.

Schmaljohn, C.S., Hooper, J.W., 2001. Bunyaviridae: the viruses and their replication. In: Bernard D.M.K., Fields, N., Bernard Roizman, Diane, E., Griffin, Malcolm, A., Martin, Robert, A., Lamb, Peter, M., Howley, Stephen, E., Straus (Eds.), Fields Virology, vol. 2. Lippincott Williams & Wilkins, Philadelphia, PA, pp. 1581–1633.

Severson, W.E., Schmaljohn, C.S., Javadian, A., Jonsson, C.B., 2003. Ribavirin causes error catastrophe during Hantaan virus replication. J. Virol. 77, 481–488.

Skibo, E.B., Meyer Jr., R.B., 1981. Inhibition of inosinic acid dehydrogenase by 8-substituted purine nucleotides. J. Med. Chem. 24, 1155–1161.

Strouse J.J., Jeselnik M., Tapaha F., Jonsson C.B., Parker W.B., Arterburn J.B., 2005. Copper-Catalyzed arylation with boronic acids for the synthesis of N^1-aryl purine nucleosides. ChemInform 36.

Sun, Y., Chung, D.H., Chu, Y.K., Jonsson, C.B., Parker, W.B., 2007. Activity of ribavirin against Hantaan virus correlates with production of ribavirin-5′-triphosphate, not with inhibition of IMP dehydrogenase. Antimicrob. Agents Chemother. 51, 84–88.

Wong, C.G., Meyer Jr., R.B., 1984. Inhibitors of inosinic acid dehydrogenase. 2-Substituted inosinic acids. J. Med. Chem. 27, 429–432.

Wright, G.E., Brown, N.C., 1990. Deoxyribonucleotide analogs as inhibitors and substrates of DNA polymerases. Pharmacol. Ther. 47, 447–497.

Yanagihara, R., Chin, C.T., Weiss, M.B., Gajdusek, D.C., Diwan, A.R., Poland, J.B., Kleeman, K.T., Wilfert, C.M., Meiklejohn, G., Glezen, W.P., 1985. Serological evidence of Hantaan virus infection in the United States. Am. J. Trop. Med. Hyg. 34, 396–399.